Published on 22 May 2018. Downloaded by Universidade Federal do Rio Grande do Sul on 7/8/2019 10:32:15 PM.

JAAS

ROYAL SOCIETY OF CHEMISTRY

TECHNICAL NOTE

View Article Online
View Journal | View Issue

Cite this: *J. Anal. At. Spectrom.*, 2018, **33**, 1269

A comparative study of sheathing devices to increase robustness in inductively coupled plasma optical emission spectrometry *via* a nitrogen flow†

Guilherme Luiz Scheffler,[a] Dirce Pozebon [a] and Diane Beauchemin *[b]

Received 26th April 2018
Accepted 22nd May 2018

DOI: 10.1039/c8ja00118a

rsc.li/jaas

Five different glass sheathing devices were used to introduce 20 mL min^{-1} N_2 sheathing gas around the effluent from the spray chamber to see the effect of their dimensions on plasma robustness as measured using the Mg II 280.270 nm/Mg I 285.213 nm emission signal ratio in inductively coupled plasma (ICP) optical emission spectrometry (OES). A clear relationship between device dimensions and the plasma robustness profile along the ICP central channel was observed. With an aerosol inlet having an inner diameter of 1.0 cm in the sheathing device, mixing of N_2 with the aerosol was minimised and the resulting sheath increased robustness, the higher thermal conductivity of N_2 *versus* Ar likely improving energy transfer between the bulk plasma and the central channel. The configuration of the outlet is also important, as any bottleneck favours mixing of N_2 with the aerosol, which in turn cools the plasma, thereby shifting the region of maximum robustness to higher above the load coil. Regardless of device dimensions, plasma robustness was always better with N_2 sheathing gas. An increased ion-to-atom emission signal ratio also resulted for other elements than Mg. The presence of N_2 also seems to affect excitation mechanisms, such as charge transfer between NO^+ and Cd or Ni, which appears to take place at higher observation height, after N_2 has had enough time to diffuse into the central channel.

Introduction

The energy coupling efficiency between the bulk plasma and its central channel, *i.e.* plasma robustness, is a key parameter in inductively coupled plasma (ICP) spectrometry to ensure adequate sample desolvation, vaporisation, atomisation and ionisation in ICP mass spectrometry (MS), as well as excitation of atoms and ions in ICP optical emission spectrometry (OES).[1–5] Even though it is well accepted that high applied radiofrequency (RF) power, low nebuliser gas flow rate and use of a wider bore injector lead to robust conditions, common negative side effects of such conditions include increased flicker noise, loss of sensitivity or excessive analyte diffusion in the central channel of the ICP.[6–9]

Plasma robustness can also be improved by adding a foreign molecular gas to the Ar ICP flow,[10–13] or as a sheathing gas around the aerosol carrier gas flow,[14] to increase energy transfer through a modification of the fundamental properties of the ICP. For example, adding a small flow of N_2 to the nebuliser gas flow using a tee improved plasma robustness, mitigated matrix effects and increased ICP excitation temperature.[15–17] The effect of the foreign gas on robustness depends on the way in which it is added to the plasma, the concurrent water load and the absolute Ar gas flow rates, in addition to the physico-chemical properties of the gas itself. Introducing it as a sheathing gas usually leads to a gas layer between the plasma ring and the central channel.[3,14]

A sheathing device was first used by Murillo and Mermet[3] to add H_2 to the ICP, thereby enhancing the local thermal conductivity and thus increasing the excitation temperature with almost no increase in continuum background, which ultimately improved detection limits. Beauchemin and Craig[17] inserted a sheathing device between the spray chamber and the torch to introduce a low N_2 flow and produce a mixed-gas Ar–N_2 ICP for ICPMS. Although it reduced sensitivity, the sheathing N_2 flow improved stability, reduced mass bias and lowered detection limits in some cases when compared to those obtained with an Ar ICP. A sheathing device may also be useful for O_2 introduction in the ICP to prevent soot deposition when organic solutions are being analysed.[18]

Since the early work of Lichte[19] who designed a torch with four gas inlets, including one for an Ar sheathing flow to facilitate the analysis of sample solutions containing a high concentration of salt, the benefits of using a sheathing flow have been recognised. However, no study has been reported on the effect of the design and dimensions of the sheathing device or on sheathing gas flow effects. The emission/ion profiles

[a]*Universidade Federal do Rio Grande do Sul, Instituto de Química, Porto Alegre, RS, 91501-970, Brazil. E-mail: guilherme.scheffler@ufrgs.br; dircepoz@iq.ufrgs.br*

[b]*Queen's University, Department of Chemistry, Kingston, ON, K7L 3N6, Canada. E-mail: diane.beauchemin@queensu.ca*

† Electronic supplementary information (ESI) available: Tables S1 and S2. See DOI: 10.1039/c8ja00118a

Published on 22 May 2018. Downloaded by Universidade Federal do Rio Grande do Sul on 7/8/2019 10:32:15 PM.

around the central channel of the ICP would provide information about the effect of the device on robustness, foreign gas diffusion or extent of mixing with the plasma Ar flow. Such data would be useful to enable an improvement of available sheathing devices. Therefore, in the current study, the ion-to-atom emission signal ratio of several elements were collected to study the diffusion of the sheathing gas into the central channel.

Experimental

Instrumentation

Measurements were carried out using a lateral-view ARCOS ICPOES instrument (SPECTRO Analytical Instruments, Kleve, Germany) equipped with a Burgener T2100 parallel path nebuliser (Burgener Research, Mississauga, ON, Canada) fitted to a baffled cyclonic spray chamber (SCP Science, Baie d'Urfé, QC, Canada). The ICPOES operating parameters are summarised in Table 1. Five different sheathing devices, shown in Fig. 1, and whose dimensions are summarised in Table 2, were compared for N_2 addition. Commercially available device 1 was compared to home-made devices 2–5. Each device was inserted between the spray chamber and the ICP torch. Emission profiles were collected by automated torch movement (controlled by software). Addition of N_2 to the plasma (outer) gas flow was done through a Y connector. Two mass flow controllers (model 1259C-01000SV, MKS Instruments Inc., Andover, MA, USA) allowed precise N_2 addition. The N_2 flow rates investigated were based on previous works,[14–16] where the minimum flow rate increasing robustness to a constant value while being tolerable in the central ICP channel was selected.

Table 1 Instrumental operating conditions for ICPOES

Parameter	Value
Radio frequency power	1.4 kW
Ar plasma gas flow rate	12.0 L min^{-1}
N_2 flow rate in the plasma (outer) gas	0.4 L min^{-1}
Ar auxiliary gas flow rate	1.0 L min^{-1}
Ar aerosol carrier gas flow rate	0.70 L min^{-1}
N_2 sheathing gas flow rate	20 mL min^{-1}
Sample uptake rate	1.0 mL min^{-1}
Observation height above the load coil (ALC)	10–20 mm
Integration time	28 s

Chemicals, standards and reference materials

Doubly deionised water (DDW) was obtained from an Arium Pro UV/DI System (Sartorius Stedim Biotech, Goettingen, Germany) and used to prepare solutions and samples. A stock multi-elemental solution (100 mg L^{-1}) was prepared in 5% v/v HNO_3 by dilution of 10 000 mg L^{-1} mono-elemental standard solutions (SCP Science, Baie d'Urfé, QC, Canada) of Al, As, Cd, Co, Cr, Cu, Fe, K, La, Li, Mg, Mn, Mo, Ni, P, Pb, S, Sb, Sc, Si, Se, Sr, Ti, V, Y, Zn and Zr. Calibration solutions ranging from 0 to 20 mg L^{-1} were prepared in 5% v/v HNO_3, by serial dilution of the stock solution. A sub-boiling distillation system (DST-1000, Savillex, Minnetonka, MN, USA) was used to purify HNO_3 and HCl (ACS grade, Fisher Scientific, Ottawa, ON, Canada) reagents. Two certified reference materials (SS1 and SS2) contaminated soils from SCP Science were analysed to demonstrate the higher accuracy and robustness with N_2. In each case, 2 mL of aqua regia (prepared 1 h before use) were added to 0.1 g of soil in a glass beaker and heated to 90 °C on a hotplate for 4 h. After cooling, the solutions were diluted to 15 mL with DDW in volumetric flasks.

Results and discussion

Preliminary optimisations of Ar–N_2 ICP

With 0.4 L min^{-1} of N_2 in the plasma gas and 20 mL min^{-1} of N_2 sheathing gas around the aerosol gas flow, the Ar plasma gas flow rate was changed from 11 to 15 L min^{-1} while monitoring the intensities of emission lines having a wide range of excitation energies. Plasma robustness, as assessed using the Mg II 280.270 nm/Mg I 285.213 nm intensity ratio, was 10, 9.95, 9.58, 9.26 and 8.86 at 11, 12, 13, 14 and 15 L min^{-1} Ar plasma gas flow rate, respectively. As robustness decreased with an increase in Ar plasma gas flow rate, so did analyte emission intensity (see

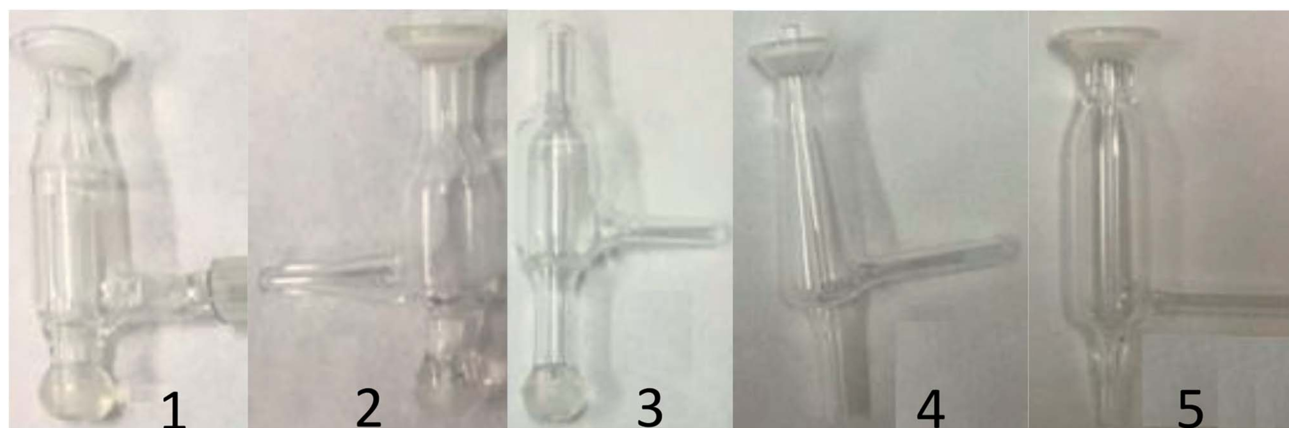

Fig. 1 Devices used to add 20 mL min^{-1} N_2 sheathing gas.

This journal is © The Royal Society of Chemistry 2018

Published on 22 May 2018. Downloaded by Universidade Federal do Rio Grande do Sul on 7/8/2019 10:32:15 PM.

Table 2 Dimensions of the devices inserted between the spray chamber and the ICP torch for N_2 addition as sheathing gas

Device	1	2	3	4	5
Length	8.0 cm	6.5 cm	7.5 cm	7.5 cm	7.5 cm
Internal diameter of aerosol tube	1.0 cm	1.0 cm	5 mm	3 mm	2 mm
Central tube length	5.0 cm	4.0 cm	5.0 cm	7.8 cm	7.5 cm
Device diameter	1.5 cm (base) to 1.0 cm (neck)	1.5 cm (base) to 1.0 cm (neck)	1.5 cm (base) to 0.5 cm (neck)	1.5 cm (base) to 1.0 cm (neck)	1.5 cm (base) to 1.0 cm (neck)

Table S1†), irrespectively of excitation energy in most cases. This is a result of the N_2 concentration decreasing in the plasma as the Ar flow rate increases, in turn decreasing the power density in the ICP. Because the ICP may extinguish (and melt the torch) when the plasma gas flow rate is as low as 11 L min^{-1}, the Ar plasma gas flow rate was kept at 12 L min^{-1} for the remainder of this work. The same flow rate was previously used on the same instrument for a mixed-gas plasma involving N_2 addition to the plasma gas and H_2 introduction as a sheath gas.[12]

Analyte emission intensities were also monitored as the auxiliary gas flow rate was increased from 0.6 to 3.0 L min^{-1}. Again, intensities and plasma robustness decreased with an increase in auxiliary gas flow rate (see Table S2†). This is due to the concurrent displacement of the analytical zone. However, when the auxiliary gas flow rate was 0.6 L min^{-1}, the ICP was unstable. To avoid plasma extinction, the auxiliary gas flow rate was fixed at 1.0 L min^{-1}. This is again consistent with that found by multivariate optimisation for the above mentioned Ar–N_2–H_2 plasma.[12]

Fig. 2 shows that, in most cases, the highest signal intensities were obtained when the nebuliser gas flow rate was 0.70 L min^{-1}. Plasma robustness (not shown) decreased as the nebuliser gas flow rate increased above this value, down to that commonly observed with an Ar ICP. Given that a similar optimum nebuliser gas flow rate was also found for devices 2 and 3, the nebuliser gas flow rate was fixed at 0.70 L min^{-1}. In Fig. 2, two atomic emission lines with low excitation energy (K I and Li I) behave differently. Given that the Li I intensity is not strongly affected by the presence of N_2 (see Table S1†), the rise in Li I intensity with an increase in nebuliser gas flow rate likely reflects the shorter residence time in the plasma, which decreases the Li II population within the observation region. In the case of K I, the signal decrease is a result of an increase in background caused by the addition of N_2.

Sheathing devices evaluation

Sheathing devices allow part of the additional gas not to mix with the nebulised aerosol flow, in contrast to adding the gas through a T or Y connection. Because the geometry and size of the sheathing device may affect the extent of mixing, different modifications were made, where the length, diameter of the aerosol inlet tube and design of the outlet were varied, as shown in Fig. 1 and detailed in Table 2. The plasma robustness criterion was used to compare the various devices shown in Fig. 1, with and without the sole addition of N_2 as sheathing gas to the ICP so as to clearly see the effect of the sheathing gas. A single set of operating conditions (listed in Table 1, except that no N_2 was added to the plasma gas) was used for the comparison, even if it was not optimal for all devices, in order to rule out the effect of other operating parameters, such as a change in sample

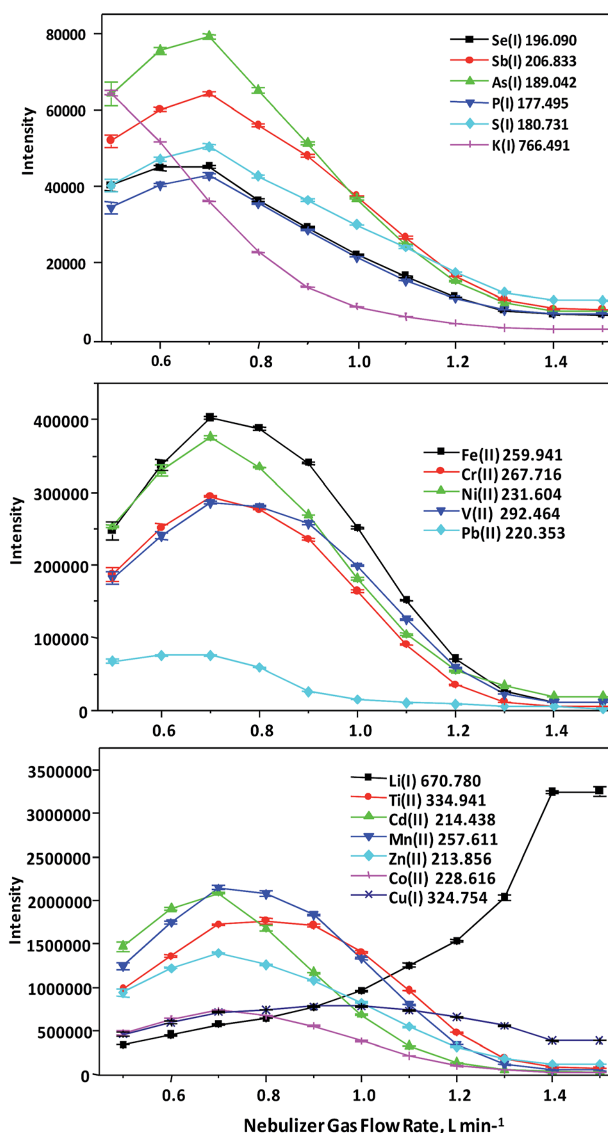

Fig. 2 Effect of the nebuliser gas flow rate on background-corrected analyte intensities measured at 10 mm ALC for a 5 mg L^{-1} multi-element solution with 400 mL min^{-1} N_2 in the plasma gas and 20 mL min^{-1} N_2 sheathing gas through device 1.

Published on 22 May 2018. Downloaded by Universidade Federal do Rio Grande do Sul on 7/8/2019 10:32:15 PM.

introduction efficiency associated with a change in aerosol carrier gas flow rate. To study diffusion of the N_2 sheath gas, the robustness was monitored at different observation heights. The results are summarised in Table 3 where, regardless of the device used and observation height, the robustness of the plasma was always better with N_2 sheathing gas.

Without N_2 sheathing gas, the maximum robustness is observed at 10 mm ALC, irrespectively of the sheathing device, except with device 2, where the maximum is at 12 mm ALC although robustness does not change much from 10 to 14 mm ALC with device 2 (as well as device 3). Given the similarities between devices 1 and 2, including in axial velocity (which should be constant, as the same aerosol carrier gas flow rate was used in all cases), this comparison reveals that even small differences in dimensions can have a very significant impact on the Ar ICP. In any case, the internal diameter of the aerosol tube in the sheathing device clearly has no effect on the observation position of maximum robustness when no sheathing gas is used.

The impact of differences in sheathing device dimensions is even more evident upon the sole addition of N_2 as a sheathing gas to the plasma. The best height for robustness is similar to that without sheathing gas with devices 1 and 2, despite the higher axial velocity that would be expected from the addition of 20 mL min^{-1} N_2 sheathing gas if thorough mixing of N_2 with the aerosol occurred. In contrast, increasing the observation height by 3–6 mm is required with N_2 sheathing gas for devices 3–5, which have a narrower internal tube. As the total axial velocity should be the same for all devices, the aerosol carrier gas and the sheathing gas flow rates being constant, the shift in position of maximum robustness due to an increase in axial velocity from N_2 addition should be independent of the device. Clearly then, the differences in position of maximum robustness between the devices can only be ascribed to the N_2 sheathing gas and differences in fluid dynamics arising from the different sheathing device designs.

The gradual decrease from 1.5 to 1.0 cm at the outlet of device 1 ensures that N_2 mostly remains around the central channel. Hence, the axial velocity of the aerosol and thus the observation height for maximum robustness remain as if no sheathing gas was present. Only an increase in robustness is observed, from the energy transfer that is likely promoted by the higher thermal conductivity of N_2 *versus* Ar. In contrast, the constant 1.0 cm length over 1.6 cm at the outlet of device 2 leads to more mixing of N_2 with Ar in the central channel, thereby increasing the apparent axial velocity of the aerosol and cooling the plasma. This results in a shift in the position of maximum robustness to slightly higher in the ICP.

The greatest shift in the position of maximum robustness is achieved with device 3 because of the higher axial velocity of the aerosol caused by the smaller diameter of the outlet, along with its longer neck, which favours mixing of N_2 with the aerosol. Judging from the shift of maximum robustness to higher ALC, some mixing of N_2 with the aerosol also seems to occur with devices 4 and 5, despite the internal tube extending outside the sheathing device. If no mixing with N_2 occurred and only a change in axial velocity was at play, then the shift would be greater with device 5 than device 4, as its aerosol tube is smaller than that of device 5. With device 4, a similar robustness is nonetheless achieved at 14 mm ALC as with device 1 at 10 mm ALC. Given that device 1 provides the highest robustness with and without N_2 sheathing gas, it was selected for subsequent studies.

Other signal ratios

Fig. 3 shows the ion-to-atom intensity ratio obtained for Cd, Cu and Ni, as well as the Ba II/Mn II ratio. The latter was monitored because it increases with the overpopulation of metastable Ar (Ar^m) species.[20,21] The Cd II/Cd I profiles in Fig. 3 suggest different excitation mechanisms in the Ar ICP and Ar–N_2 ICP. In particular, the increase of the ratio at greater distances ALC in the Ar–N_2 ICP may be caused by charge transfer with NO^+

Table 3 Plasma robustness (Mg II 280 nm/Mg I 285 nm emission intensity ratio) at different observation heights ALC without (the sheathing gas inlet was sealed) and with 20 mL min^{-1} N_2 sheathing gas using the devices in Fig. 1 (without addition of N_2 to the plasma gas flow), where the maximum robustness is highlighted in each case

Observation height ALC, mm	Sheathing device									
	1		2		3		4		5	
	With N_2	Without N_2	With N_2	Without N_2	With N_2	Without N_2	With N_2	Without N_2	With N_2	Without N_2
10	8.08	5.12	7.12	3.68	5.33	3.47	7.61	4.20	6.67	3.99
11	7.86	4.64	7.14	3.73	5.33	3.46	7.57	4.14	7.07	3.97
12	6.98	4.46	7.50	3.78	5.74	3.47	7.64	4.07	7.33	3.92
13	7.34	4.27	7.53	3.73	5.96	3.44	7.91	4.00	7.45	3.85
14	6.66	4.07	7.47	3.73	6.11	3.42	8.07	3.87	7.41	3.79
15	6.55	3.71	7.33	3.61	6.26	3.31	7.68	3.82	7.40	3.74
16	6.52	3.36	7.14	3.50	6.31	3.23	7.08	3.69	7.16	3.65
17	6.77	3.32	6.84	3.38	6.20	3.15	6.88	3.55	6.96	3.55
18	6.22	3.59	6.61	3.29	6.06	3.06	6.61	3.46	6.64	3.42
19	5.40	3.19	6.26	3.19	5.93	2.97	6.26	3.33	6.29	3.31
20	4.96	2.91	5.89	3.11	5.64	2.90	6.02	3.26	6.04	3.21

 This journal is © The Royal Society of Chemistry 2018

Published on 22 May 2018. Downloaded by Universidade Federal do Rio Grande do Sul on 7/8/2019 10:32:15 PM.

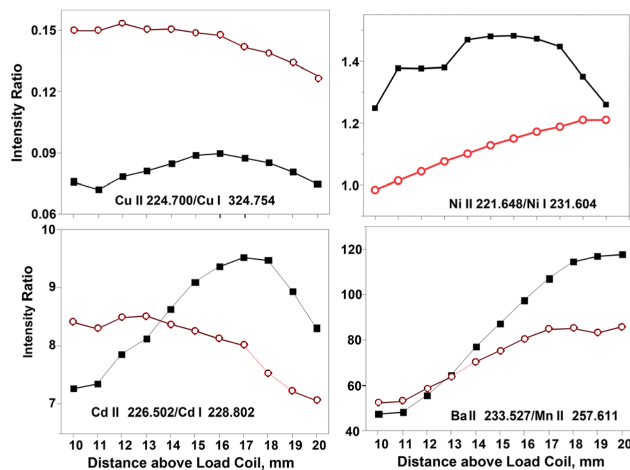

Fig. 3 Selected signal ratios at different observation heights ALC (without N_2 in the plasma gas flow) without (red open circles) and with (black full squares) 20 mL min^{-1} N_2 sheathing gas added using device 1.

(ionisation energy = 9.26 eV), which promotes the ionisation of Cd (ionisation energy = 8.99 eV). The same process likely explains the difference between the Ni II/Ni I ratio profiles with and without N_2. The Cu ratio anomaly, where the ratio in the Ar–N_2 ICP is systematically lower than that in an Ar ICP, corroborate previous results obtained when a low flow of N_2 was added to the ICP.[16] The addition of N_2 may induce an overpopulation of Ar^m, which decreases the Cu ion population, thereby increasing that of Cu atoms. This phenomenon is lesser in the Ar ICP because the amount of N_2 present (from atmospheric air entrainment and HNO_3 present in the solution) is much lower. With respect to the Ba II/Mn II ratio, the increase of Ba II may result from the energy closeness of Ba II (11.21 eV) to that of Ar^m (11.55 eV). The fact that similar excitation mechanisms were observed when the same quantity of N_2 was introduced through a T device[16] seems to indicate that they are independent of the device type, *i.e.* sheathing device or T, and mostly depend on the foreign gas entering the ICP.

Conclusions

The robustness of the ICP was improved with 20 mL min^{-1} N_2 sheathing gas irrespectively of the sheathing device dimensions. However, those dimensions have a great impact on plasma robustness, as they may affect the axial velocity of the aerosol and the extent of mixing with N_2 as well as any energy transfer from the bulk plasma to the central channel that may be promoted by the high thermal conductivity of N_2, drastically affecting the analytical characteristics of the resulting ICP. The higher robustness is also reflected by emission signal ratios of other elements. Future studies will include modifications of device 1 to improve the performance of electrothermal vaporisation (ETV) coupled to ICPOES. Aerosol pre-evaporation, like was previously done to simultaneously introduce water vapour with the ETV effluent to increase plasma robustness,[22] will also be tested to eliminate condensation in the device, which constitutes its main problem.

Conflicts of interest

There are no conflicts to declare.

Acknowledgements

The authors gratefully acknowledge the financial support of the National Science and Engineering Research Council of Canada (grant number 39487-2013) and Anglo American Pty for the donation of the ARCOS ICPOES instrument. GLS received a CNPq scholarship in Canada (201398/2015-0) while DP is grateful for a CNPq research fellowship in Brazil.

References

1 J.-M. Mermet, *Spectrochim. Acta, Part B*, 1989, **44**, 1109–1116.
2 J.-M. Mermet, *Anal. Chim. Acta*, 1991, **250**, 85–94.
3 M. Murillo and J.-M. Mermet, *Spectrochim. Acta, Part B*, 1989, **44**, 359–366.
4 D. Beauchemin, *Mass Spectrom. Rev.*, 2010, **29**, 560–592.
5 M. Murillo and J.-M. Mermet, *Spectrochim. Acta, Part B*, 1987, **42**, 1151–1162.
6 J.-M. Mermet, *Anal. Chim. Acta*, 1991, **250**, 85–94.
7 X. Romero, E. Poussel and J.-M. Mermet, *Spectrochim. Acta, Part B*, 1997, **52**, 487–493.
8 J. W. Tromp, M. Pomares, M. Alvarez-Prieto, A. Cole, H. Ying and E. D. Salin, *Spectrochim. Acta, Part B*, 2003, **58**, 1927–1944.
9 H. P. Longerich, B. J. Fryer, D. F. Strong and C. J. Kantipuly, *Spectrochim. Acta, Part B*, 1987, **42**, 75–92.
10 Y. Makonnen and D. Beauchemin, *Spectrochim. Acta, Part B*, 2014, **99**, 87–93.
11 Y. Makonnen and D. Beauchemin, *Spectrochim. Acta, Part B*, 2015, **103–104**, 57–62.
12 Y. Makonnen, W. R. MacFarlane, M. L. Geagea and D. Beauchemin, *J. Anal. At. Spectrom.*, 2017, **32**, 1688–1696.
13 S. M. Burchell, MSc thesis, Queen's University, 2000.
14 G. L. Scheffler and D. Pozebon, *J. Anal. At. Spectrom.*, 2015, **30**, 468–478.
15 G. L. Scheffler and D. Pozebon, *Spectrochim. Acta, Part B*, 2015, **113**, 84–92.
16 G. L. Scheffler, C. A. Martins and D. Pozebon, *J. Anal. At. Spectrom.*, 2016, **31**, 1141–1149.
17 D. Beauchemin and J. M. Craig, *Spectrochim. Acta, Part B*, 1991, **46**, 603–614.
18 D. Hausler, *Spectrochim. Acta, Part B*, 1987, **42**, 63–73.
19 F. E. Lichte, A. L. Meier and J. G. Crock, *Anal. Chem.*, 1987, **59**, 1150–1157.
20 X. Romero, E. Poussel and J. M. Mermet, *Spectrochim. Acta, Part B*, 1997, **52**, 487–493.
21 X. Romero, E. Poussel and J. M. Mermet, *Spectrochim. Acta, Part B*, 1997, **52**, 495–502.
22 N. Sadiq, L. Huang, F. Kaveh and D. Beauchemin, *Food Chem.*, 2017, **237**, 1–6.

Electronic Supplementary Material (ESI) for Journal of Analytical Atomic Spectrometry.
This journal is © The Royal Society of Chemistry 2018

Please do not adjust margins

ARTICLE

Table S1. Influence of the plasma (outer) gas flow rate on emission lines intensities for a solution containing 5 mg L^{-1} of the elements; 400 mL min^{-1} N_2 and 20 mL min^{-1} N_2 were respectively added to the plasma and nebulizer gas flows.

Wavelengths	Energy*, eV	11 L min^{-1}	12 L min^{-1}	13 L min^{-1}	14 L min^{-1}	15 L min^{-1}	Ratio 11/15
Se I 196.090	6.32	72000±840	63900±600	54700±650	49200±300	44000±400	1.63
Sb I 206.833	5.98	82600±770	75300±340	66820±580	61730±150	57000±400	1.45
As I 189.042	6.56	107400±1400	96700±830	83550±860	75330±340	67700±500	1.58
P I 177.495	6.99	60100±700	53640±560	46470±270	42000±370	38000±300	1.58
S I 180.731	6.85	68400±630	62150±640	54450±600	50000±300	45840±250	1.49
K I 766.491	1.62	31700±450	26900±500	22340±290	19350±180	17000±190	1.86
Li I 670.780	1.85	774600±4500	760400±13900	734500±4300	726200±680	712700±5300	1.08
Fe II 259.941	13.09	628000±3000	579660±9500	524800±5500	488000±5800	452900±2300	1.38
Cr II 267.716	12.95	457500±3900	422000±4400	378300±2500	348500±3700	319700±2400	1.43
Ni II 231.604	14.03	605600±5000	542000±6000	472400±3000	423600±6100	380760±3600	1.59
V II 292.464	11.37	437300±3700	408400±5300	375600±3200	354100±2900	331000±1900	1.32
Pb II 220.353	14.79	103300±1600	88800±1200	73780±940	64000±460	56100±550	1.84
Ti II 334.941	10.56	2572800±19000	2435000±36000	2289000±18000	2198000±18000	2090000±28000	1.23
Cd II 214.438	14.77	3300000±21000	2861550±47000	2388000±33000	2106000±36000	1809000±29000	1.82
Mn II 257.611	12.25	3312000±26000	3068000±46000	2792000±28000	26167000±23000	2420000±34000	1.37
Zn II 213.856	15.51	1812000±12000	1658000±23000	1493000±11000	1392000±16000	1288000±13000	1.40
Co II 228.616	13.70	1190100±10300	1077000±11000	948600±7200	858000±11000	777900±7000	1.53
Cu I 324.754	3.82	938400±6600	911000±15000	869000±5000	854400±4500	831800±1600	1.13
Mg II 280.270	12.07	8216000±41000	7650000±110000	6909000±51000	64435000±66000	5907000±83000	1.39
Mg I 285.213	4.34	808600±6000	768700±9300	721100±4500	695400±4700	666100±1200	1.21

*Obtained from https://www.nist.gov/pml/atomic-spectra-database, which lists the excitation energy for atomic lines and the sum of the excitation and ionization energies for ionic lines.

Please do not adjust margins

Please do not adjust margins

Table S2. Influence of the auxiliary gas flow rate on emission lines intensities for a solution containing 5 mg L^{-1} of the elements; 400 mL min^{-1} N_2 and 20 mL min^{-1} N_2 were respectively added to the plasma and nebulizer gas flows.

Wavelength, nm	3.0 L min^{-1}	2.5 L min^{-1}	2.0 L min^{-1}	1.5 L min^{-1}	1.0 L min-^{1}	0.6 L min^{-1}	Ratio 1.0/3.0
Se I 196.090	38000±350	42157±800	49000±300	56700±280	62710±500	65800±400	1.65
Sb I 206.833	42500±400	48650±800	57700±200	67000±390	74500±400	78900±400	1.75
As I 189.042	53680±670	61000±1000	72500±600	85000±700	95000±450	99800±800	1.76
P I 177.495	34260±150	37200±700	42500±200	48500±250	53000±200	55100±300	1.54
S I 180.731	40900±470	43000±700	48600±450	55250±300	60800±280	63800±800	1.48
K I 766.491	14800±70	15700±100	17800±160	21500±700	26100±200	28150±800	1.76
Li I 670.780	931900±960	846200±6500	825700±2450	801600±22100	764700±4300	750800±6400	0.82
Fe II 259.941	338000±3000	401300±60000	483500±2500	547600±6900	582000±5700	600000±4700	1.72
Cr II 267.716	229200±950	279400±3800	341400±2600	391300±5200	419400±5000	432500±6700	1.82
Ni II 231.604	256600±2000	320000±5200	403200±4300	478600±4400	537600±7300	562300±12000	2.09
V II 292.464	260800±1200	303200±3100	356300±2400	394000±6000	411200±4200	419300±6400	1.57
Pb II 220.353	30960±300	41600±1200	56400±100	73200±1100	87300±400	96200±1200	2.82
Ti II 334.941	1723000±37000	1939600±24900	2267720±11000	2427000±35000	2455000±26000	2487000±33000	1.42
Cd II 214.438	1088700±8600	1365600±21700	1883500±13900	2389000±26000	2794000±100000	3038000±25000	2.56
Mn II 257.611	1784000±39000	2107400±26500	2606480±16900	2920000±21000	3064000±52000	3150000±33000	1.71
Zn II 213.856	955700±9400	1084600±19200	1291800±9900	1486300±1600	1637830±33000	1740000±17000	1.71
Co II 228.616	535400±4300	660400±9600	822400±8300	964300±10000	1073000±13000	1117000±19000	2.00
Cu I 324.754	778100±300	804500±7500	877450±4000	917000±19000	915000±8000	912000±10000	1.17
Mg II 280.270	4325000±83000	5168000±71000	6401450±37750	7208000±70000	7500000±1200000	7680000±99000	1.74
Mg I 285.213	494700±1000	571000±5500	669600±4300	740300±10000	772000±8000	783000±10000	1.56
Mg II 280/Mg I 285	8.74±0.16	9.05±0.12	9.56±0.05	9.73±0.09	9.77±0.16	9.80±0.12	-

This journal is © The Royal Society of Chemistry 20xx

Please do not adjust margins